# ORIGINAL PAPER

**Keunjoo Kim · Hong Seub Kim · Jae Yon Kim**
**Young Hee Lee · Hyung Jae Lee**
**Hwack Joo Lee · Hyun Ryu**

# Solid-state interdiffusion mechanism in strained $Si_{1-x}Ge_x$/Si heterostructures

**Abstract** The interdiffusion in a low-strained $Si_{0.93}Ge_{0.07}$/Si epilayer was analyzed by double-crystal X-ray diffraction. The interdiffusion was characterized by a low diffusion barrier of 1.81 eV with a diffusion constant of $4.3 \times 10^{-5}$ cm$^2$/sec, which indicates correlation with the stacking fault generated by the homoepitaxial growth of the Si layer prior to the growth of the strained SiGe layer. At the very low-strained layer, the driving force causing the interdiffusion is the concentration gradient, and the mechanism is self-diffusion of Si. Furthermore, the interdiffusion mechanisms were classified into three groups, depending on the Ge mole fraction $x$. For $x < 0.2$, the diffusion process in the SiGe alloy is similar to a self-diffusion of Si atoms, while, for $0.2 < x < 0.4$, Ge atoms prefer to be diffused out from the alloy. Finally, for $x > 0.4$, Si atoms can be diffused into the alloy.

## Introduction

Strained SiGe/Si heterostructures are essential in device applications using band gap engineering on Si-based technology. Considerable achievements were reported on electrical devices such as heterojunction bipolar transistors (HBT) [1] and high electron mobility transistors (HEMT) [2]. For the fabrication of such kinds of devices, band gap narrowing and band offset are utilized, resulting in compositional gradient and strain at heterointerfaces. The interfacial abruptness is one of the most important device factors. However, since high-temperature annealing is included in device processes, the thermal treatment causes strain relaxation and forms a natural diffusion system due to a compositional gradient across SiGe/Si interface. The intermixing alters the interfacial properties and impairs device performance. The strain relaxation and the interdiffusion are closely related to each other because both are related to the activation energy.

The interdiffusion process is very complicated and sensitive to the quality of the samples. It even depends on the experimental methods of sample growth and measurement. Tracer diffusion analysis is useful for the measurement of the diffusion constant in a relatively high-temperature annealing process [3]. The transition of the diffusion mechanism from interstitial to vacancy with increasing Ge concentration was confirmed in the case of Ge diffusion in SiGe [4]. Based on Rutherford backscattering spectrometry (RBS), Holländer et al. [5] suggested that under tensile stress, interdiffusion is correlated with the interstitial mechanism for the Si layers on an Si/SiGe superlattice symmetrically grown on relaxed SiGe. Cowern et al. [7] determined the local diffusion behavior from the high-resolution depth profile by secondary-ion mass spectroscopy (SIMS). They suggested that interdiffusion in an Si-rich SiGe layer under compressive strain is mediated by vacancy. This shows that the interstitial pathway of interdiffusion is favored under tensile strain or high thermal stress at relatively high annealing temperatures, and the vacancy pathway is dominant under compressive strain at a relatively low annealing temperature.

Strain relaxation and interdiffusion were also investigated by photoluminescence (PL) for very thin SiGe alloy films [6]. The PL emission energy shift induced by post-annealing provides information on the diffusion constant and the activation energy. The energy shift reflects that the profile of the electrostatic potential at the heterointerface can be modulated because of interdiffusion. Another useful experimental method is double-crystal X-ray diffraction (DCXD) analysis [8–11].

K. Kim (✉) · H.S. Kim · J.Y. Kim · Y.H. Lee · H.J. Lee
Department of Physics and Semiconductor Physics Research
Center, Jeonbuk National University, Jeonju 560-756, Korea

H.J. Lee · H. Ryu
Korea Research Institute of Standards and Science,
Taejon 305-600, Korea

By annealing pseudomorphically strained samples at different temperatures for various annealing times, the diffusion constant and the activation energy can be determined by the measurement of the integrated intensity decay of DCXD peaks resulting from composition modulation. In spite of these extensive studies, the physical mechanism for enhanced interdiffusion is still incomplete, and systematic investigation is urgently required.

In this work, the interdiffusion process was investigated by DCXD measurement in a very Si-rich $Si_{1-x}Ge_x$ alloy with a Ge mole fraction of $x = 0.07$. The relationship between interdiffusion and strain relaxation was discussed on the basis of the interpretation of scattered X-ray intensity and the full width at half maximum (FWHM). The normalized X-ray intensity was implemented in order to estimate the activation energy in the diffusion process. The quality of the sample was evaluated by high-resolution transmission electron microscope (HRTEM). Finally, from available experimental results, the nature of the interdiffusion mechanism was discussed.

## Experimental method

The undoped and low-strained $Si_{0.93}Ge_{0.07}$ epitaxial layers having 2000 Å thickness were grown on Si(001) by solid-source molecular-beam epitaxy (MBE) at 730 °C after homoepitaxial growth of an Si layer with the thickness of 2000 Å using a temperature gradient from 950 to 730 °C. This growth temperature gives two-dimensional planar growth of the strained layer for $x = 0.07$ [12] and is high enough to remove point defects. It is useful to note that the plasticity temperature for bulk silicon is 600 °C [13], which implies that the homoepitaxial growth at the high temperature may cause built-in thermal relaxation of the growth fault and introduce localized dislocations rather than point defects. The strained layer is thermodynamically metastable and is fairly marginal to the critical thickness of the epilayer according to the theory of Kim and Lee [14].

The morphology of an as-grown film was investigated by an HRTEM (H9000-NAR) at 300 kV with a point resolution of 1.8 Å. The samples were also annealed in the temperature range of 750–900 °C in dry ambient nitrogen in a quartz tube. The DCXD measurements were made using Cu $K_\alpha$ radiation, and the diffraction peak was observed on the symmetric (004) Bragg reflection plane. The integrated intensity decays of the X-ray peak were determined for the annealed samples at different temperatures for different amounts of time. The integrated DCXD intensity was then normalized based on the weight of each piece so as to eliminate variations due to the sample size. The normalized intensities were fitted in order to obtain the activation energy and the diffusion constant.

## Results and discussion

Figure 1 shows the typical DCXD rocking curves for the symmetric (004) Bragg reflection plane using Cu $K_{\alpha 1}$ radiation on samples annealed for 5 min. The as-grown sample shows the well-defined thickness fringes from the abrupt interface. On increasing the annealing temperature, the fringes faded out gradually and disap-
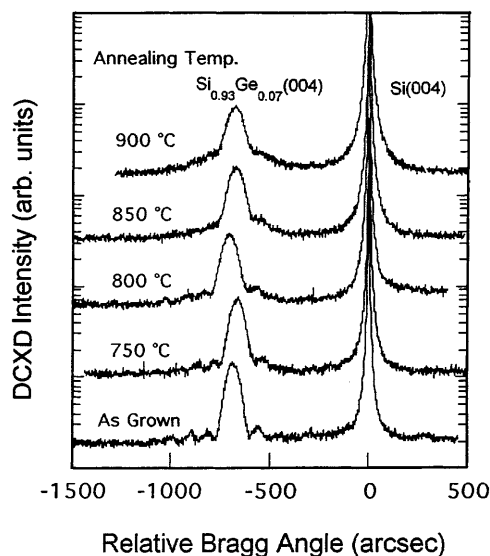


**Fig. 1** DCXD intensities on the strained sample of $Si_{0.93}Ge_{0.07}$/Si interface. The as-grown sample shows clear fringes near the SiGe peak. On increasing the annealing temperature, the fringes are smeared out due to interdiffusion at the strained interface. At a temperature of 800 °C the DCXD peak of the SiGe (004) plane obviously shifts to the higher angle, indicating the increase of Ge concentration

peared completely in the samples annealed over 850 °C, indicating the broadened interfacial layer due to interdiffusion. The DCXD peak position of the $Si_{0.93}Ge_{0.07}$ (004) plane slightly shifts to the increased Ge composition at a high annealing temperature (800 °C). This indicates that a high temperature is associated with the interdiffusion related to the strain relaxation which causes the change of Ge mole fraction. Interdiffusion without any severe strain relaxation was also confirmed from the DCXD measurement for the (115) asymmetric reflection plane, which gives consistent results.

Figure 2 shows the decay of the integrated intensity of the X-ray diffraction as a function of the annealing time. On lowering the temperature, the decay rate of the intensity is increased in the early stage of annealing and then gradually becomes saturated for the further process. For the sample annealed at 900 °C, however, the prolonged annealing shows a jump with the elevated intensity. This may indicate that the structural change at the SiGe/Si interface has happened. The degradation of the interface gives the large value of the FWHM, while the intensity decreases.

Figure 3 shows the intensity as a function of the FWHM. The normalized intensity decreases in the early stage of annealing (STAGE 1) and then the intensity is not decreased any more with increasing FWHM (STAGE 2). Since the generation of dislocations makes many reflection planes, the integrated intensity increases while the FWHM is broadened by inhomogeneity [16]. The sample annealed for a long time at a temperature of 900 °C provides the very broad FWHM extended into STAGE 2. This indicates that the hidden
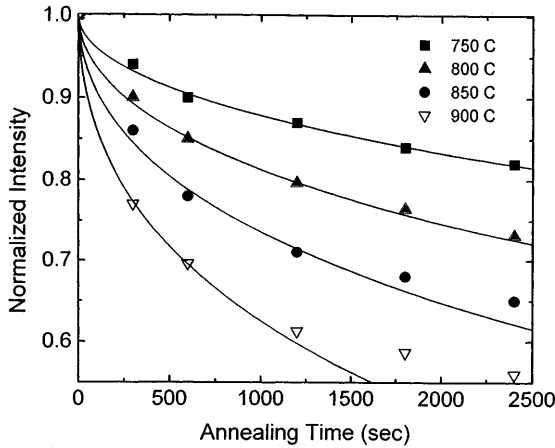
**Fig. 2** The normalized intensity of DCXD with respect to the annealing time. On increasing the annealing time, overall intensities decay because of the interdiffusion process. For the prolonged annealing process at the high temperature of 900 °C, the intensity is enhanced because of film degradation due to introduction of the dislocation effect

stacking faults are related to this phenomenon and activated by the thermal energy. The activation energy required for the dislocation-enhanced diffusion process is about 2.0 eV [15].

The X-ray intensity is affected by several factors such as polarization, structure, Lorentz multiplicity, absorption, and temperature [16, 17]. After annealing, Si and Ge interdiffuse across the interface. The interdiffusion changes the structural factor and affects the diffracted beam intensity. The change of the structural factor is expressed in terms of the atomic form factors of Si and Ge atoms and the changed mole fraction of Ge at the interface. The change of the mole fraction is correlated with the changed Ge concentration causing the Ge diffusion due to the annealing effect.

The integrated DCXD intensity [$I(t)$] of the first-order satellite as a function of annealing time for different

temperatures was normalized by the integrated intensity of the as-grown sample ($I_0$). The relative X-ray intensity of the annealed sample to that of the as-grown sample is expressed by the relationships of the solid-state diffusion process [17, 18]:

$$\frac{\mathrm{d}}{\mathrm{d}t}\ln\left(\frac{I(t)}{I_0}\right) = -\frac{p}{2}\left(\frac{D}{\pi t}\right)^{1/2} \tag{1}$$

$$D(T) = D_0 \exp(-E_A/k_B T) \tag{2}$$

$$p = \frac{32}{|F_0|}\frac{\mu\alpha x f_{\mathrm{Ge}}}{1 - \exp(-\mu\alpha\tau)} \tag{3}$$

$$F_0 = 8\{(1-x)f_{\mathrm{Si}} + x f_{\mathrm{Ge}}\} \tag{4}$$

where $F_0$ is the structural factor on the as-grown sample with respect to the (004) reflection plane, $\mu$ the mass absorption coefficient of the epilayer, $\alpha = \frac{1}{\sin\gamma} + \frac{1}{\sin\beta}$, $\gamma$ the angle between the epilayer and the incident beam, $\beta$ the angle between the epilayer and the diffracted light beam, $f_{\mathrm{Si}}(f_{\mathrm{Ge}})$ atomic form factors for Si(Ge), $\tau$ the thickness of the epilayer, and $t$ the annealing time. This formula is applicable for the single-layered film under the condition that the thickness of film is large enough to be comparable with the diffusion length localized around the interface. Note that the decay of the intensity is related to the explicit function of the annealing time instead of the periodicity in the multilayered film [9].

The diffusivity in SiGe can be evaluated in the above expression of the Arrhenius form. As shown in Fig. 4, a diffusion constant and an activation energy are obtained with the values $D_0 = 4.3 \times 10^{-5}$ cm$^2$/sec and $E_A = 1.81 \pm 0.20$ eV, respectively. This activation energy for the diffusion process is lower than that of the dislocation formation energy (from the strain relaxation of 2.0 eV) [15]. However, it is valuable to note that the self-diffusion of Si requires an activation energy of
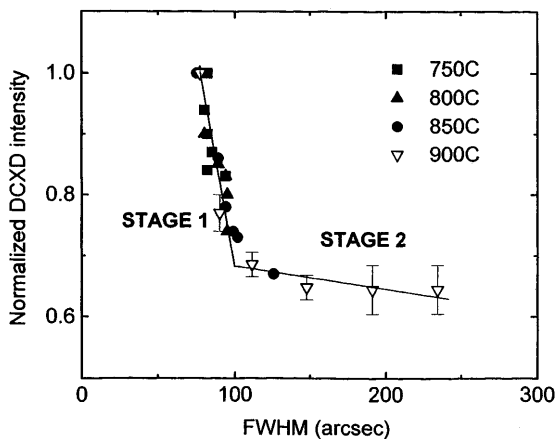


**Fig. 3** The normalized DCXD intensity as a function of the FWHM, showing two stages: the strain-related interdiffusion (STAGE 1) and the dislocation-enhanced interdiffusion (STAGE 2)
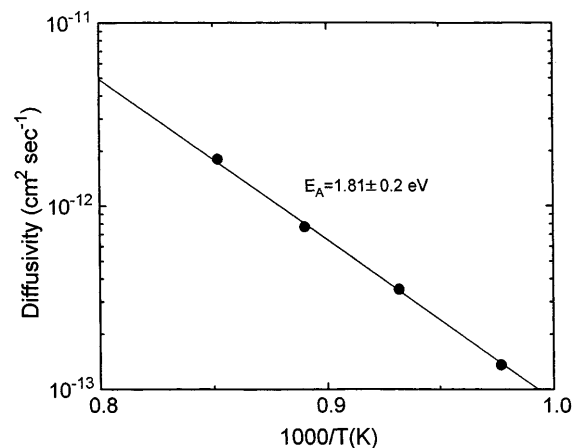


**Fig. 4** The Arrhenius plot of the diffusivity, indicating an activation energy of 1.81 eV for $x = 0.07$. The diffusion constant $D_0 = 4.3 \times 10^{-5}$ cm$^2$/sec was found

1.86 eV through the interstitial channel without the dislocation effect [4, 19].

From available literature, the activation energies for various Ge mole fraction $x$ are shown in Fig. 5. Of course, exact comparability is not possible because of different growth conditions, but useful information on the relationship between the diffusion barrier and the strain is provided. The mechanism of interdiffusion is categorized into three groups: self-diffusion of Si (Group I), Ge diffusion in Si-rich SiGe (Group II), and Si diffusion into Ge-rich SiGe alloys (Group III). Most of the values in Group I, for a Ge mole fraction $x < 0.2$, are slightly greater than those for the self-diffusion of Si, where an activation energy of 1.86 eV is required [19]. The value lower than the self-diffusion energy indicates the dislocation-loop-enhanced diffusion process [15, 21]. The driving force of the interdiffusion in Group I is mainly the concentration gradient, partially perturbed by a small strain effect.

Group II is located in the range $0.2 < x < 0.4$, and the process requires a large activation energy similar to that of Ge diffusion in Si. The activation energy for Ge diffusion in SiGe is close to the activation energy of 4.0–5.3 eV [4, 9, 10, 22, 23] required for Ge diffusion in Si. It is valuable to note that Ge diffusion in Si shows a transition from vacancy-mediated diffusion with an activation energy of 4.1 eV at temperatures below 1050 °C to interstitial-mediated diffusion with an energy of 5.3 eV at temperatures above 1100 °C [24] and the mixed phase of substitutional-interstitial interchange and vacancy mechanisms at intermediate temperatures [10, 23]. Cowern et al. [7] suggested that in the range of the Ge mole fraction $0.1 < x < 0.3$ and below the temperature of 1050 °C, Ge diffusion in SiGe alloy is dictated by vacancy-dominant diffusion kinetics with activation energy increasing linearly with Ge composi-

tion, $E_{SiGe}[Ge] = E_{Si}[Ge] + 1.68x$. However, as illustrated in Fig. 5, the diffusion kinetics are not simple, because the diffusing species depends on the mole fraction of SiGe alloys according to the minimization of the energy of the systems.

In Group III, where $x > 0.4$, the Si atom as the diffusing species with the lower activation energy is preferred to the Ge atom to be diffused. This conjecture may be demonstrated by atomistic energy calculations on the diffusion system. However, it is obvious that the activation energy for the Si diffusion into SiGe is larger than 3 eV [3, 4, 9], which is the energy required for Si diffusion in unstressed Ge. Under a strong compressive misfit stress, the formation of the interstitial defect, which is related to the outward breathing of lattice relaxation, is strongly suppressed [25]. Therefore, the interdiffusion process is enhanced by vacancy formation by inward breathing of lattice relaxation for the Si diffusion into Ge-rich SiGe alloys.

In addition to the strain effect perturbed by point-defect formation, the dislocation-loop formation is sometimes correlated with the strain relaxation and severely affects the interdiffusion kinetics, which are also closely related to the annealing temperature. In order to understand the quality of the as-grown sample of $Si_{0.93}Ge_{0.07}/Si$ epilayer, the TEM image was obtained (Fig. 6). The morphology of the MBE-grown epilayer includes spots of dislocation with a size of 300 Å at the homoepitaxial Si layer. The spot is overlaid by diffraction contrast arising from the strain field of the crystal defect. The homoepitaxial layer of Si was grown on the Si surface with RCA cleaning ($H_2SO_4$ for organic materials and $HF : H_2O_2 = 1 : 4$ for the native oxide layer) and baking that native oxide layer at 950 °C. The Si layer was grown atomic layer by atomic layer with a growth rate of 1 Å/sec up to 1000 Å in MBE by lowering the growth temperature from 950 to 730 °C. The temperature was then fixed at 730 °C both for the last Si layer (1000-Å thick) and for the SiGe layer (2000-Å thick). Although there is no strain energy in homoepitaxy, the thermal gradient induces thermal instability, causing the crystal defect.

The defect consists of extrinsic stacking faults bound by partial dislocations at their ends (A, B, C, and D) taken in the HRTEM mode with [110] zone axis as shown in Fig. 6b. The HRTEM image of a (111) oriented Si crystal contained an L-shaped extended dipole generated by the interaction of split dislocations. The partial dislocations directed to $\langle 111 \rangle$, $\langle 100 \rangle$, and $\langle \bar{1}\bar{1}1 \rangle$, and steps in the direction of $\langle \bar{1}\bar{1}1 \rangle$ with the angle of 11.2° were observed. The one- or two-monolayer steps are separated by the increased intervals of 3–15 monolayers in the growth direction. This can be explained by the step model of Schwoebel and Shipsey [20], according to which the activation energy of diffusion for an Si atom jumping over the edge of a step from the terrace above is higher than that for jumping into the step from a site in front of the step on the same level. They have shown that this step model leads to an array of equally
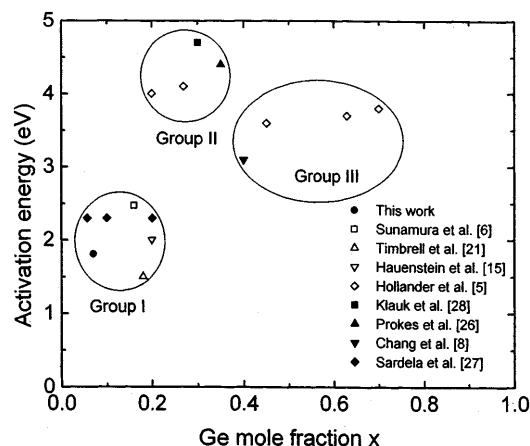


Fig. 5 The activation energy in terms of the Ge mole fraction. The energy is classified into three groups: self-diffusion of Si below $x = 0.2$ driven by the concentration gradient (Group I), Ge diffusion from SiGe in the range of $x = 0.2$–0.4 mediated by the vacancy under compressive stress (Group II), and Si diffusion into SiGe alloys above $x = 0.4$ (Group III)
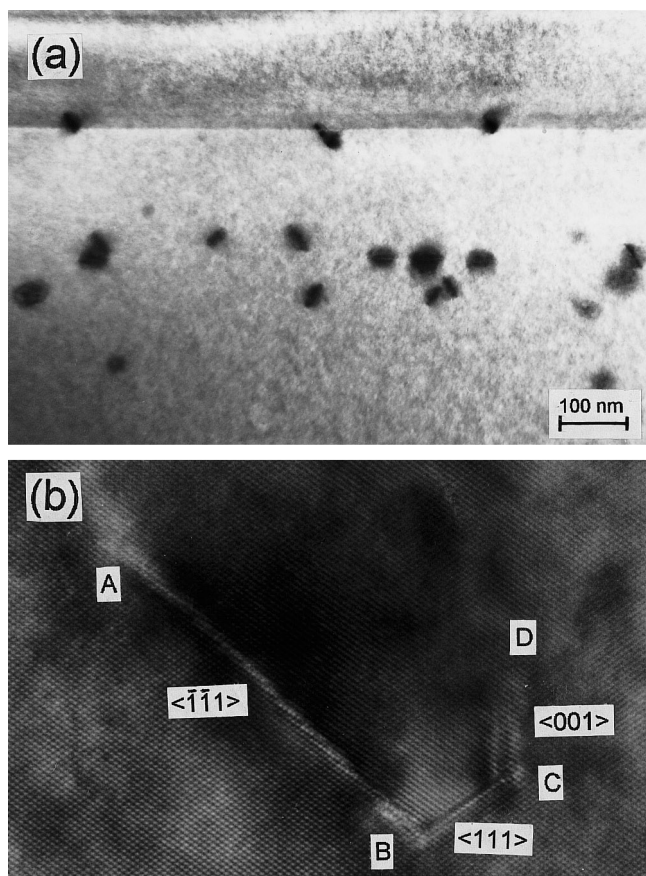
**Fig. 6 a** TEM image on the as-grown Si$_{0.93}$Ge$_{0.07}$/Si layer and **b** HRTEM image on one of the spots shown in **a**. The 300-Å-sized spots are mainly distributed on the homoepitaxial Si layer of 2000 Å and a few spots are also found in the interface. The pre-existing stacking fault is bound by partial dislocations directed to $\langle 001 \rangle$, $\langle 111 \rangle$, and $\langle \bar{1}\bar{1}1 \rangle$

found to be of $4.3 \times 10^{-5}$ cm$^2$/sec and $1.81 \pm 0.20$ eV, respectively. The low strain component does not have much effect on the interdiffusion process, but the small distribution of stacking faults at the interface lowers the diffusion barrier.

In the very low-strained system, the driving force on the interdiffusion is the concentration gradient, and the process is similar to the self-diffusion of Si by the interstitial route. This group extends up to $x = 0.2$, with an activation energy of about 1.8–2.3 eV. Under considerable compressive strain, for the range of Ge composition $0.2 < x < 0.4$, the interdiffusion follows the pathway of the Ge diffusion in the Si-rich SiGe alloy by mediating the vacancy defect for the experimental data performed below a temperature of 1000 °C. The activation energy for this second group is leveled to a value of 4–5 eV. For interdiffusion in the Ge-rich SiGe alloy where $x > 0.4$, under high compressive strain, the diffusion species changes to Si atoms. The interdiffusion process in this third group requires an activation energy of 3–4 eV. In conclusion the interdiffusion mechanism depends on the strain effect in terms of Ge mole composition. However more study, based on atomistic calculations, is desirable to support the Si diffusion process into the Ge-rich SiGe alloy.

spaced steps. However, the TEM image shows that the steps at the bottom propagate faster due to the gradient of the growth temperature of the Si layer. In the early stage of annealing, stacking faults at the interface lower the diffusion barrier slightly. However, prolonged annealing causes strongly enhanced interdiffusion because of the correlation with the dislocation effect.

## Conclusions

In summary, the interdiffusion process was investigated for a low-strained interface by X-ray diffraction, and the structural morphology of the strained film was investigated by TEM. Most dislocations are distributed on the homoepitaxial layer because of the gradient of the growth temperature which varied from 950 to 730 °C. Few localized dislocations were found at the interface of the SiGe epilayer. From the DCXD analysis for the MBE-grown Si$_{0.93}$Ge$_{0.07}$ alloy on the Si layer, the diffusion constant and the activation energy were

## References

1. Temkin H, Bean JC, Antreasyan A, Leibenguth R (1988) Appl Phys Lett 52: 1089
2. Schaffler F, Tobbeen D, Herzog H-J, Abstreiter G, Holländer B (1992) Semicon Sci Technol 7: 260
3. Räisänen J, Hirronen J, Anttila A (1981) Solid-State Electron 24: 333
4. McVay GI, Ducharme AR (1974) Phys Rev B 9: 627
5. Holländer B, Butz R, Mantl S (1992) Phys Rev B 46: 6975
6. Sunamura H, Fukatsu S, Usami N, Shiraki Y (1993) Appl Phys Lett 63: 1651
7. Cowern NEB, Zalm PC, van der Sluis P, Gravesteijn DJ, de Boer WB (1994) Phys Rev Lett 72: 2585
8. Chang SJ, Wang KL, Bowman RC, Adams PM (1989) Appl Phys Lett 54: 27
9. Baribeau J-M, Pascual R, Saimoto S (1990) Appl Phys Lett 57: 1502
10. Fahey P, Iyer SS, Scilla GJ (1989) Appl Phys Lett 54: 843
11. Theiss SD, Spaepen F, Aziz MJ (1996) Appl Phys Lett 68: 1226
12. Bean JC, Sheng TT, Feldman LC, Fiory AT, Lynch RT (1984) Appl Phys Lett 44: 102
13. Fiory AT, Bean JC, Hull R, Nakahara S (1985) Phys Rev B 31: 4063
14. Kim K, Lee YH (1995) Appl Phys Lett 67: 2212
15. Hauenstein RJ, Clemens BM, Miles RH, Marsh OJ, Croke ET, McGill TC (1989) J Vac Sci Technol B 7: 767
16. Cullity BD (1978) Elements of X-ray diffraction, 2nd edn. Addision-Wesley, New York, p 122
17. Chaudhuri J, Shah S, Harbison JP (1989) J Appl Phys 66: 5373
18. Kim HS (1997) Ph D thesis, Jeonbuk National University, Chonju, Korea, p 38
19. Wijaranakula W (1990) J Appl Phys 67: 7624

226

20. Schwoebel RL, Shipsey EJ (1966) J Appl Phys 37: 3682
21. Timbrell PY, Baribeau J-M, Lockwood DJ, McCaffrey JP (1990) J Appl Phys 67: 6292
22. Dorner P, Gust W, Predel P, Roll U (1984) Phil Mag 49: 557
23. Fahey P, Griffin PB, Plummer JD (1989) Rev Mod Phys 61: 289
24. Hettich G, Mehren H, Maier K (1978) In: Albany JH (ed) Defects and radiation effects in semiconductors Inst Phys Conf Series 46, Institute of Physics, London, p 500
25. Antonelli A, Bernholc J (1990) Mater Res Soc Symp Proc 163: 523
26. Prokes SM, Wang KL (1990) Appl Phys Lett 56: 2628
27. Sardela Jr MR, Hansson GV (1995) J Vac Sci Technol A 13: 314
28. Klauk H, Jackson TN (1996) Appl Phys Lett 68, 1975